# Potent Fluorinated Agelastatin Analogues for Chronic Lymphocytic Leukemia: Design, Synthesis, and Pharmacokinetic Studies

E. Paige Stout,[†] Michael Y. Choi,[§,⊥] Januario E. Castro,[§,⊥] and Tadeusz F. Molinski*[,†,‡]

[†]Department of Chemistry and Biochemistry, [‡]Skaggs School of Pharmacy and Pharmaceutical Sciences, [§]Moores Cancer Center, and [⊥]School of Medicine, University of California, San Diego, 9500 Gilman Drive, La Jolla, California 92093-0358, United States

S *Supporting Information*

ABSTRACT: Chronic lymphocytic leukemia (CLL) is the most common lymphoid neoplasia in Western societies and is currently incurable. Multiple treatment options are practiced, but the available small molecule drugs suffer from dose-limiting toxicity and undesirable side effects. The need for new, less toxic treatments is a pressing concern. Here, we demonstrate that (−)-agelastatin A (**1a**), a pyrrole-imidazole alkaloid obtained from a marine sponge, exhibits potent in vitro activity against primary cell lines of CLL and disclose the synthesis of several analogues that are equipotent or exceed the potency of the natural product. The novel synthetic analogue, 13-debromo-13-trifluoromethyl agelastatin A (**1j**), showed higher activity than the natural product when tested against the same cell lines and is the most potent agelastatin derivative reported to date. A detailed in vitro structure−activity relationship of **1a** in CLL compared to that of 22 synthetic analogues is described along with preliminary in vivo pharmacokinetic and metabolism studies on the most potent compounds.
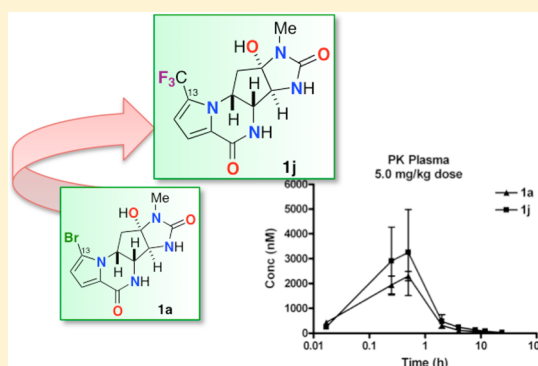
INTRODUCTION

Leukemia and lymphoma account for approximately 9% of new cancer cases diagnosed in the United States each year.[1] Chronic lymphocytic leukemia (CLL), the most common lymphoid neoplasia, progresses rapidly in two-thirds of diagnosed patients with a relatively poor prognosis. It remains an "incurable disease."[2] Current treatments of CLL include immunotherapeutic[3] and chemotherapeutic approaches. Chemotherapy treatments for CLL employ the nitrogen mustards bendamustine, chlorambucil, cyclophosphamide, and the nucleoside analogue fludarabine (Figure 1). Adverse side effects of these
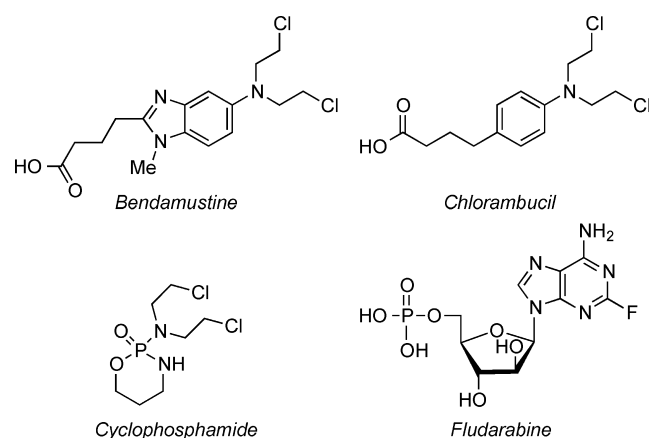
agents include nausea, fever, vomiting, diarrhea, immunosuppression, and myelotoxicity. The growing number of patients with resistant or relapsed disease with current treatments[4] presses for the development of new chemotherapeutic agents for CLL.

Agelastatins A and B (**1a,b**) are potent cytotoxic natural products isolated from the marine sponges *Agelas dendromorpha* and *Cymbastela* sp.[5] Agelastatins, including the analogues agelastatins C (**2a**) and D (**2b**),[5c] are members of the chemically diverse pyrrole-imidazole alkaloids (PIA).[6] Since Weinreb's ground-breaking total synthesis of (±)-**1a**,[7] several additional syntheses, both of the racemic compound (±)-**1a**[8a−c] and the natural antipode (−)-**1a**,[8d,e] have been achieved.[8f] Compound **1a** has been shown to inhibit the growth of in vitro cultured KB nasopharyngeal tumor cells (IC$_{50}$ 0.5−1 μg mL^{-1}), suppress osteopontin-mediated malignant transformation by β-catenin inhibition,[9] and inhibit the expression of glycogen synthase kinase (GSK-3b).[10] In a preliminary disclosure,[11] we showed that **1a** exhibits p53-independent submicromolar activity against CLL (EC$_{50}$ 60−100 nM). An early study of structure−activity relationships (SAR) of **1a** by Pietra and colleagues[5a,b] concluded that structural modifications of the OH and NH groups in rings B−D of the parent molecule were not tolerated, but more recent work by Li reveals that certain substitutions in the pyrrolecarboxamide moiety (ring A) of **1a** retain activity.[12] Here, we disclose expanded SAR mapping and

Figure 1. Structures of FDA approved CLL treatments.

Scheme 1. Synthesis of Agelastatins 1b, 1n–p, and 4a,b[a]
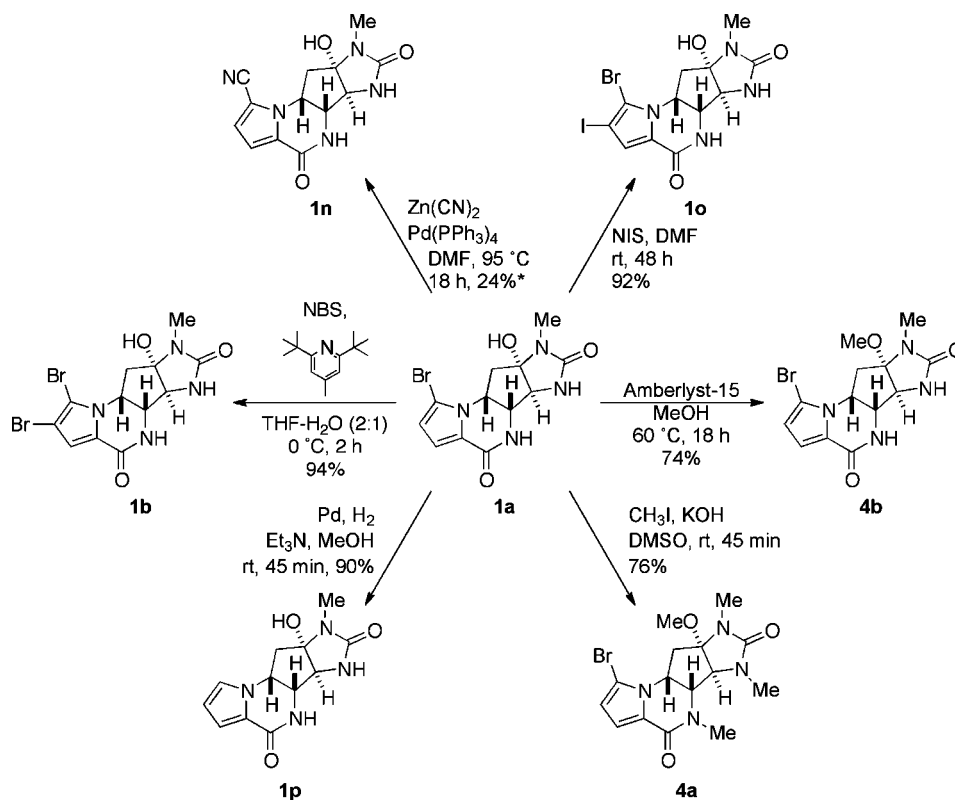
[a]*, based on recovered starting material. Compounds **1a,b,p** and **4a** were earlier reported by Pietra and coworkers.[5b] Compound **4b**, the product of the transacetalization of **1a** with MeOH, has been named agelastatin E by Mourabit and co-workers.[24]
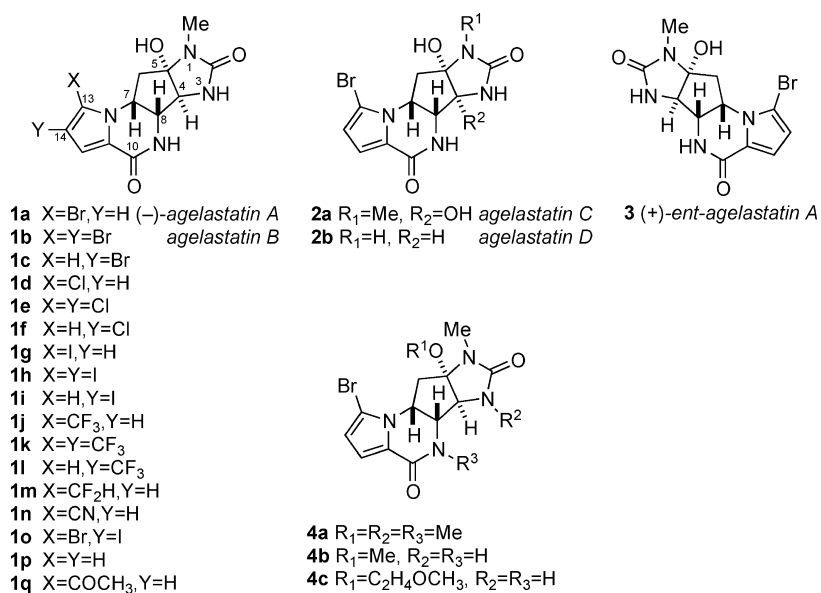

1a X=Br,Y=H (–)-*agelastatin A*	**2a** R$_1$=Me, R$_2$=OH *agelastatin C*
1b X=Y=Br *agelastatin B*	**2b** R$_1$=H, R$_2$=H *agelastatin D*
1c X=H,Y=Br	**3** (+)-*ent-agelastatin A*
1d X=Cl,Y=H	
1e X=Y=Cl	
1f X=H,Y=Cl	
1g X=I,Y=H	
1h X=Y=I	
1i X=H,Y=I	
1j X=CF$_3$,Y=H	
1k X=Y=CF$_3$	
1l X=H,Y=CF$_3$	
1m X=CF$_2$H,Y=H	
1n X=CN,Y=H	
1o X=Br,Y=I	
1p X=Y=H	
1q X=COCH$_3$,Y=H	

4a R$_1$=R$_2$=R$_3$=Me
4b R$_1$=Me, R$_2$=R$_3$=H
4c R$_1$=C$_2$H$_4$OCH$_3$, R$_2$=R$_3$=H

Figure 2. Structures of natural agelastatins (**1a,b** and **2a,b**), *ent*-(+)-agelastatin A (**3**), and synthetic agelastatins (**1c–q** and **4**[5]).

pharmacokinetic (PK) and metabolism studies of **1a** that define the most potent analogues of the agelastatin family reported to date with a predictive analysis for more potent analogues with improved PK properties.

■ **RESULTS**

Chemistry. Natural products (−)-agelastatins A (**1a**), C, and D (**2a,b**) were isolated in our laboratory from the Western

Australian sponge *Cymbastela* sp. as described elsewhere.[5c] Compounds **1b**, **1p**, and **4a,b**, respectively, were derived from natural or synthetic (−)-**1a** by simple chemical reactions according to previously described protocols (Scheme 1). Debromo-agelastatin A (**1p**), a key starting material for ring A substitution reactions, was first prepared by Pietra and co-workers by conjugate reduction−elimination of **1a** (LiAlH$_4$ and THF, 60%). In our hands, an improved yield of **1p** could be

realized by the hydrogenolysis of **1a** (H_2, Pd−C, Et_3N, and MeOH, 75−90%). The new analogues **1d−1p** (Figure 2) were all obtained utilizing known or modified reaction conditions. Agelastatin analogues **1c** and **1f−1o** represent novel compounds. Attempted synthesis of **1d−1f** under conventional chlorination reaction conditions (N-chlorosuccinimide, CH_3CN) failed to deliver product. Free radical electrophilic aromatic substitution of **1p** (N-chlorosuccinimide, $(BzO)_2$, and CCl_4)[13] also failed, most likely due to the limited solubility of **1p** in the solvent. Optimized conditions, using an alternative radical-substitution protocol (N-chlorosuccinimide, $K_2S_2O_8$, and H_2O, 1 h, 80 °C) compatible with aqueous solvent, led to clean consumption of starting material and production of the chlorinated analogues **1d−1f** as the only observed products that were readily separated by HPLC. Radical-trifluoromethylation was attempted under the conditions of MacMillan[14] but gave only a mixture of uncharacterized decomposition products. In contrast, trifluoromethylation and difluoromethylation of **1p** following the protocol of Baran and co-workers[15] (^tBuOOH, aqueous $NaSO_2CF_3$, or $ZnSO_2CHF_2$, respectively) smoothly converted the starting material to the fluorinated analogues **1j−1l** and **1m**, respectively. Attempted difluoroethylation of **1p** using similar conditions (^tBuOOH, aqueous $NaSO_2CF_2CH_3$) was unavoidably accompanied by hydrolysis giving the 13-acetyl derivative **1q**.[16]

Activities against CLL Patient and ATCC Leukemia Cell Lines. Agelastatins **1−4** were screened in assays against primary leukemia cells obtained from patients with CLL (CLL1−CLL6) obtained through the CLL Research Consortium, in addition to the immortalized leukemic JVM-2 cell line (Tables 1−3). Because of the usual variability of primary patient CLL cells, HeLa was used as a comparative standard cell

Table 1. Antitumor Activity of Natural and Synthetic Agelastatins 1a−1p with Modifications on the Pyrrole Ring

cmpd	X^a	Y	in vitro cytotoxicity EC_{50} $(\mu M)^b$			
			$CLL1^c$	$CLL2^c$	$JVM-2^d$	HeLa
1a	Br	H	0.31	0.16	0.28	0.11
1b	Br	Br	26.3	4.46	3.53	3.61
1c	H	Br	19.4	9.22	71.5	9.07
1d	Cl	H	0.95	0.32	0.20	0.63
1e	Cl	Cl	1.56	0.52	0.28	0.60
1f	H	Cl	35.9	6.05	5.33	5.16
1g	I	H	5.96	0.73	2.62	1.18
1h	I	I	26.4	96^e	49.0	262^f
1i	H	I	25.5	94.9^g	222^h	0.061
1j	CF_3	H	0.43	0.064	0.66	0.15
1k	CF_3	CF_3	$-^i$	19.2^j	41^k	153
1l	H	CF_3	45.1	4.68	22.8	19.6
1m	CHF_2	H	13.0	5.44	4.66	4.01
1n	CN	H	11.1	0.71	38.0	3.40
1o	Br	I	211	48.2	161.9^l	86.7
1p	H	H	541	3.90	120	61.5
Flu^m			17.1^n	2.66	10.4	16.0

^{a}See Figure 2 for the substituent key. ^{b}Standard error (SE) is ±0.01 μM for all data points unless otherwise noted. ^{c}CLL1 and CLL2 = CLL patient cell lines. ^{d}JVM-2 = ATCC leukemia cell line. ^{e}SE ± 2 μM. ^{f}SE ± 1 μM. ^{g}SE ± 0.2 μM. ^{h}SE ± 1 μM. ^{i}NT = not tested. ^{j}SE ± 0.1 μM. ^{k}SE ± 2 μM. ^{l}SE ± 0.2 μM. ^{m}Flu = fludarabine; see Figure 1 for the chemical structure. ^{n}Flu EC_{50} values >10 μM are considered Flu-resistant CLL strains.

Table 2. Antileukemic Activity of Select Natural and Synthetic Agelastatins against Various CLL Patient-Derived Cell Lines

cmpd	X^a	Y	in vitro cytotoxicity EC_{50} $(\mu M)^b$			
			$CLL3^c$	$CLL4^c$	$CLL5^c$	$CLL6^c$
1a	Br	H	0.24	0.37	0.29	1.15
1d	Cl	H	3.80	1.98	0.34	2.20
1e	Cl	Cl	0.98	4.42	2.02	7.50
1g	I	H	6.61	3.04	3.06	12.9
1j	CF_3	H	3.04	0.33	28.4	0.65
1n	CN	H	8.37	8.41	4.79	0.84
Flu^d			0.35	0.64	0.16	1.60

^{a}See Figure 2 for the substituent key. ^{b}Standard error is ±0.01 μM for all data points. ^{c}CLL3−CLL6 = CLL patient cell lines. ^{d}Flu = fludarabine; see Figure 1 for the chemical structure.
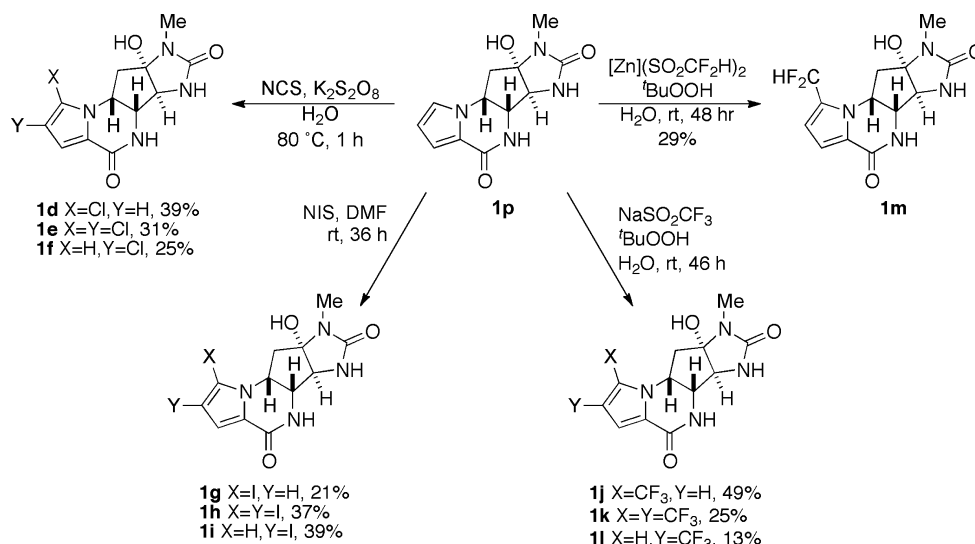
Table 3. Antitumor Activity of Natural Agelastatins (2a,b) and Synthetic Analogues (3 and 4) against CLL and HeLA Tumor Cell Lines

cmpd	antitumor EC_{50} $(\mu M)^a$			
	CLL1	CLL2	JVM-2	HeLa
2a	84.6	10.0	4.07	7.63
2b	91.1	29.0	13.2	13.7
3	$-^b$	$>1^c$	$-^b$	$-^b$
4a	140	47.7	55.7	59.0
4b	867	28.8	429	91.4
4c	$-^b$	9.39	21.1	$-^b$
Flu^d	17.1^e	2.66	10.4	16.0

^{a}Standard error is ±0.01 μM for all data points. ^{b}NT = not tested. ^{c}Compound **3** was sample limited and only tested up to 1 μM. ^{d}Flu = fludarabine; see Figure 1 for the chemical structure. ^{e}Flu EC_{50} values >10 μM are considered Flu-resistant CLL strains.

line. Several modified agelastatins showed nanomolar activity against patient CLL cells, and **1j** exhibited slightly higher potency than the natural product agelastatin A (**1a**) (CLL2 EC_{50} values 0.064 ± 0.01 μM and 0.16 ± 0.01 μM, respectively, Table 1). Any chemical modifications outside of the pyrrole ring (e.g., N- and O-methylation of **1a** to **4a,b**; Table 3) resulted in significant losses in activity, consistent with previously reported SAR data.[5]

Modifications on the pyrrole ring of agelastatin A and activity in models of primary brain tumors and CNS penetration have been recently reported;[12] however, in the present context of CLL, we have expanded the inventory of analogues and showed important influences of substituent electronegativity and size at C-13 (Scheme 2). Moving an electronegative halogen or CF_3 group from C-13 to C-14 consistently abrogated activity (CLL2 EC_{50} = 0.16 ± 0.01 μM for **1a** compared with 9.22 ± 0.01 μM for **1c**; Table 1), while reductive removal of Br from C-13 (13-debromo-agelastatin A, **1p**) also resulted in significant loss (25-fold) of activity. Interpretation of these collective data supports the importance of an electronegative functional group at position C-13 for CLL activity. The 13,14-dichloro analogue **1e** only showed a slight decrease in potency when compared to the 13-monochloro derivative **1d** (EC_{50} = 0.52 ± 0.01 μM and 0.32 ± 0.01 μM, respectively; Table 1). However, other 13,14-dihalogenated and 13,14-di-CF_3 compounds showed a much larger loss in potency when compared to that of their respective 13-monosubstituted analogues (e.g., pairwise comparisons of **1a** and **1b**; **1g** and **1h**; and **1j** and **1k**). Interestingly, the

Scheme 2. Synthesis of Pyrrole-Modified Agelastatins 1d–1m[a]

1d X=Cl,Y=H, 39%
1e X=Y=Cl, 31%
1f X=H,Y=Cl, 25%

1g X=I,Y=H, 21%
1h X=Y=I, 37%
1i X=H,Y=I, 39%

1j X=CF₃,Y=H, 49%
1k X=Y=CF₃, 25%
1l X=H,Y=CF₃, 13%

1m

1p

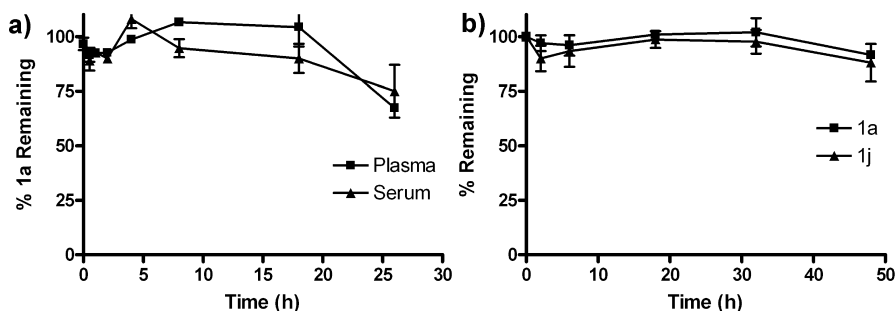[a]Compounds **1d** and **e** were independently reported by Li and coworkers.[12]

Figure 3. Stability of (a) agelastatin A [(−)-**1a**] in mouse plasma and serum and (b) **1a** and 13-debromo-13-trifluoromethyl-agelastatin A [(−)-**1j**] in human AB serum ($n = 3$, error bars indicate standard error). Concentrations of (−)-**1a** and **1j** were determined by LCMS.

difluoromethyl analogue **1m** displayed a significant loss of activity when compared to that of the trifluoromethyl derivative **1j** (CLL2 EC$_{50}$ = 5.44 ± 0.01 μM and 0.064 ± 0.01 μM, respectively, Table 1). The CHF$_2$ group, a lipophilic hydrogen bond donor,[15b] appears to induce an unfavorable interaction when located at C-13.

Stereochemistry was also shown to play an essential role in CLL activity. Of the two enantiomers of **1a** (Table 3), only the natural antipode (−)-**1a** exhibited nanomolar activity (EC$_{50}$ 110–310 nM); unnatural *ent*-agelastatin A (+)-**3** is essentially inactive (EC$_{50}$ >1000 nM), suggesting chiral constraints at the cognate binding site of the natural product, perhaps underscoring the importance of the 3D disposition of NH and OH H−bond donor−acceptors in the structure of (−)-**1a**.

Stability in Mouse and Human Plasma. Nonspecific protein binding of **1a** and **1j** was relatively low. Compounds **1a** and **1j** were recovered in 65−90% yields from both mouse plasma and human serum after 24 h of incubation (Figures 3 and S29, Supporting Information). Experimentally measured physical properties of **1a** and **1j**, including water solubility and log P (Table 4) suggest that **1a** and **1j** are appreciably stable but possibly rapidly excreted by glomerular filtration, which limits the achievable $t_{1/2}$ in serum and plasma.

In Vivo Studies in Mice: Pharmacokinetic Properties of 1a and 1j. Agelastatin A (**1a**) was administered as a single dose (2.5 mg/kg) to female BALB/c mice under both

Table 4. Measured and Calculated Physical Properties of 1a and 1j

property	1a	1j
solubility (H$_2$O)[a]	0.64 mg/mL	0.30 mg/mL
log P[a]	0.18	0.78

[a]Measured at 25 °C.

intravenous (IV) and intraperitoneal (IP) routes (Figure 4) and monitored by time-dependent plasma levels. Initial plasma uptake of **1a** was much greater with IV administration; however, other pharmacokinetic (PK) parameters (Table 5) favored IP administration. Consequently, subsequent PK studies were performed using IP administration. Comparing administrations of **1a** and **1j** to mice at a single dose (2.5 or 5.0 mg/kg, Figure 5), the area under the curve (AUC) and C$_{max}$ significantly favored **1j** over **1a**, while the half-lives ($t_{1/2}$) of the two compounds (Table 6) were similar. The improved PK properties of **1j** may be due to the more favorable log P value when compared to those of **1a**.

Phase I/II Metabolism Model: Agelastatin A Analogues. Mouse and human microsomes were separately incubated with **1a** or **1j** and monitored for metabolism by cytochrome P450 enzymes. After 1 h of incubation with microsomal fractions, quantitative recovery (LCMS) of both **1a** and **1j** from samples of the supernatant was achieved under
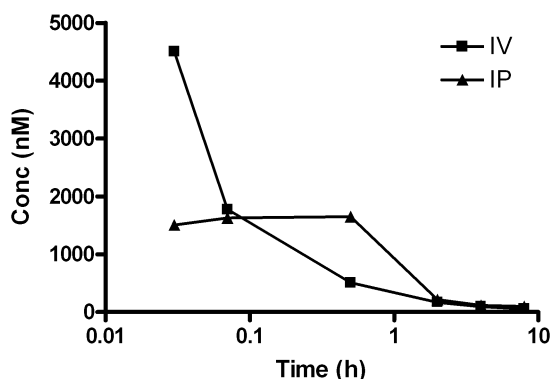
Figure 4. Plasma concentration–time curves for (−)-agelastatin A [(−)-**1a**] after a single 2.5 mg/kg dose using both IV and IP administration routes. Concentrations of (−)-**1a** were determined by LCMS.

Table 5. Pharmacokinetic Parameters of Agelastatin A (1a) Based on a Single 2.5 mg/kg Dose, Intravenous (IV) or Intraperitoneal (IP)

PK parameter	administration route	
	intravenous (IV)	intraperitoneal (IP)
AUC[a]	1742	2946
C_{max}[b]	4.50 μM	1.65 μM
T_{max}[c]	2 min	30 min
$t_{1/2}$[d]	4 min	1 h

[a]AUC = area under the curve. [b]C_{max} = maximum compound concentration. [c]T_{max} = time at which C_{max} occurs. [d]$t_{1/2}$ = compound half-life. PK parameters were calculated in GraphPad Prism software.

conditions that metabolized the positive control, 7-ethoxycoumarin[17] (Supporting Information, Figure S30). Under similar conditions, debromoagelastatin A (**1p**) was incubated with a near quantitative recovery, suggesting the metabolic stability of the 4-ring system of the agelastatins. Select phase II metabolism of **1a** was briefly explored using both mouse and human S9 fractions. No formation of glucoronides was detected after the incubation of **1a** with glucuronidase,[18] an observation that militates against the involvement of phase II pathways in the clearance of **1a**.

Collectively, these data suggest that **1a** and analogues are not competent substrates for Cyp oxidative modification or glucuronidation. Although we cannot at this time exclude sulfation of the tertiary OH group or direct excretion through other routes (feces or bile), some evidence was obtained for

Table 6. Pharmacokinetic Parameters of 1a and 1j[a]

PK parameter[b]	2.5 mg/kg dose		5.0 mg/kg dose	
	1a	1j	1a	1j
AUC	6260	12 925	4294	6508
C_{max}	1.28 μM	4.18 μM	2.30 μm	3.25 μM
T_{max}	30 min	15 min	30 min	30 min
$t_{1/2}$	1.4 h	1.2 h	1 h	45 min

[a]Parameters calculated from LCMS analysis of time-course monitoring of blood samples after single 2.5 or 5.0 mg/kg IP dose. [b]See caption in Table 4 for the key.

urinary excretion. Treatment of mice with **1a** (2.5 mg/kg, IP), followed by collection and single-drop urinalysis (5 min) and analysis revealed a 217 μM concentration of only unmetabolized **1a** compared to that of the control (Supporting Information, Figure S31). These data are consistent with rapid excretion of **1a** in mice through glomerular filtration, although follow-up studies are warranted to fully understand the total metabolism–excretion of **1a**.

■ DISCUSSION AND CONCLUSIONS

Five synthetic analogues (**1d**, **1e**, **1g**, **1j**, and **1n**) exhibited nanomolar in vitro activity against CLL patient cells, with comparable potency to the natural product (−)-agelastatin A (**1a**). Only substitutions on the pyrrole ring at C-13 were tolerated, suggesting a very narrow SAR window for this class of compounds. The remarkable activity of trifluoromethyl analogue **1j** suggests that an electron-withdrawing group at C-13 is desirable and that similarly sized isosteres of the Br substituent found in natural **1a** may be tolerated. The Hammett σ_{meta} constants[19] for Br, CHF$_2$, and CF$_3$ are 0.39, 0.29, and 0.43,[20a] respectively, while Taft steric constants $-E_S$ are 1.16, 1.91, and 2.40,[20b] respectively (Table 7). Comparisons of cytotoxic activities (Table 1−3) suggest that an electron-withdrawing group is required at C-13 for potent activity and that groups as large as CF$_3$ (comparable to *i*-Pr) are tolerated. We predict analogues that subscribe to these criteria may also be expected to exhibit significant activity.[21] The chlorinated analogues **1d** and **e** were also recently reported by Li and co-workers;[12] however, the present work expands the repertoire of active agelastatins and presents the first examples of halogenated agelastatins substituted by CF$_3$ and I.

Compounds **1a** and **1j** exhibit in vitro stability in mouse and human plasma, but time course measurements reveal rapid clearance of both compounds from the blood, most likely due
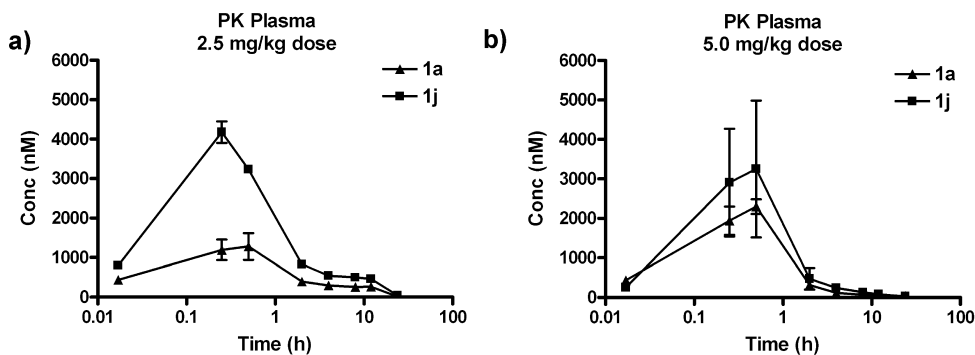

Figure 5. Plasma concentration–time curves for (−)-agelastatin A (**1a**) and 13-debromo-13-trifluoromethyl-agelastatin (**1j**) after a single (a) 2.5 or (b) 5.0 mg/kg dose (*n* = 4, error bars indicate standard error). Concentrations of (−)-**1a** and **1j** were determined by LCMS.

Table 7. Selected Hammett and Taft Parameters for Agelastatin Analogue Substituents

group	σ_{meta}[a]	$-E_s$[b]
CH_3	−0.07	1.24
$CH(CH_3)_2$		1.71
CH_2F	0.12	1.48
CHF_2	0.29	1.91
CF_3	0.43	2.40
Cl	0.37	0.97
Br	0.39	1.16
I	0.35	

[a]From ref 20a. [b]From ref 20b. See ref 20c for a modified scale of $-E_S$ values.

to efficient excretion; a phenomenon that may be related to their relatively low log P values (0.18 and 0.78, respectively; Table 4). Future efforts will focus on expanding a wider window of SAR through the synthesis of additional C-13-substituted agelastatin analogues that subscribe to predictive steric and electron-withdrawing effects, while aiming to improve PK properties, particularly log P, and retention of high potency.

■ EXPERIMENTAL SECTION

General Procedures. Reagent-grade chemicals were used as purchased. Dry CH_3CN and DMF were dried by passage through double dry alumina cartridges and molecular sieves, respectively, under an atmosphere of Ar. ^1H and 2D NMR spectra were acquired using a Bruker spectrometer equipped with a 1.7 mm {$^{13}C,^{15}N$}^1H micro-cryoprobe operating at 600 MHz; a Jeol spectrometer equipped with a 2 channel $^1H,^{19}F${$^{15}N,^{31}P$} inverse-detect probe operating at 500 MHz (^1H) or 470 MHz (^{19}F); or a Varian XSens ^{13}C{^1H}cryoprobe probe operating at 125 MHz spectrometer. ^1H and ^{13}C NMR spectra were acquired in CD_3OD and referenced to δ 3.31 and 49.0 ppm, respectively. CD spectra were measured on samples in 0.2 cm quartz cells recorded with a Jasco 810 spectropolarimeter at 23 °C. IR spectra were obtained using a Jasco FT-IR-4100 FTIR spectrometer equipped with a ZnSe ATR plate. High-resolution mass spectra were recorded using an Agilent 6230 TOF mass spectrometer equipped with an Agilent 1200 microflow HPLC. Semipreparative and preparative HPLC separations were carried out using a dual-pump instrument equipped with a high-dynamic range UV−vis detector set to λ 280 nm. All solvents used for HPLC purification were redistilled in glass from commercial HPLC grade solvents. Retention times (t_R) are reported in minutes. Low-resolution LCMS analyses were conducted with a Thermo-Finnigan Accela-MSQ instrument operating in ESI mode with a Phenomenex Kinetex C_{18} column (150 × 4.6 mm, 2.6 μm), using gradient mobile phases of aqueous CH_3CN with 0.1% formic acid at 0.7 mL min^{-1}. All compounds used in biological assays were analyzed by LCMS and conformed to purities of ≥95%.

(−)-Agelastatin A (1a). Natural (−)-agelastatin A used in the present study was isolated from the Australian sponge *Cymbastela* sp. collected in Western Australia as previously described.[5c] Enantiopure synthetic (−)-1a, received as a generous gift from Professor Justin Du Bois (Stanford University),[22] was repurified by reversed-phase HPLC prior to use (Luna phenyl−hexyl, 250 × 10 mm, 5 μm; linear gradient from 20−40% aqueous CH_3CN over 20 min, 2.5 mL min^{-1}) to afford (−)-1a (>99% ee) and the minor byproduct 1c. NMR and MS data for (−)-1a matched previously reported data.[5] ^1H NMR (500 MHz, CD_3OD) δ 6.91 (d, *J* = 4.1 Hz, 1H), 6.33 (d, *J* = 4.1 Hz, 1H), 4.60 (dt, *J* = 12, 6.3 Hz, 1H), 4.09 (d, *J* = 5.5 Hz, 1H), 3.88 (s, 1H), 2.81 (s, 3H), 2.65 (dd, *J* = 13, 6.4 Hz, 1H), 2.10 (t, *J* = 12.6 Hz, 1H) ppm.

(−)-Agelastatin B (1b). *N*-Bromosuccinimide (NBS, 5.0 mg, 28 μmoL, 1.1 equiv) was added in one portion to a stirred solution of (−)-agelastatin A (1a, 9.1 mg, 27 μmoL, 1 equiv), and 2,6-di-*tert*-butyl-4-methylpyridine (8.3 mg, 41 μmoL, 1.5 equiv) in water (0.5 mL) and

THF (1.0 mL) at 0 °C. After 2 h, the reaction was quenched by the addition of a mixture of $Na_2S_2O_3$ (satd, aq) and $NaHCO_3$ (satd, aq) solution (1:1, 100 μL). The aqueous solvent was removed under reduced pressure and the residue purified by preparatory reversed-phase HPLC (Duragel C_{18}, 20 × 50 mm, 5 μm; linear gradient from 10−40% aqueous CH_3CN over 25 min, 10 mL min^{-1}), to yield pure (−)-agelastatin B (1b, 10.7 mg, 94%) as a white solid with NMR and MS spectra that matched previously reported data.[5a] ^1H NMR (500 MHz, CD_3OD) δ 6.97 (s, 1H), 4.60 (dt, *J* = 12.2, 6.2 Hz, 1H), 4.11 (d, *J* = 5.6 Hz, 1H), 3.88 (s, 1H), 2.81 (s, 3H), 2.68 (dd, *J* = 13.1, 6.4 Hz, 1H), 2.12 (app-t, *J* = 12.6 Hz, 1H) ppm of HRTOFMS [M − H]$^-$ *m/z* 416.9209 (calcd for $C_{12}H_{11}N_4O_3Br_2$, 416.9203).

13-Debromo-14-bromo-agelastatin A (1c). Compound 1c was isolated as a minor product from the repurification of synthetic (−)-agelastatin A (1a). ^1H NMR (600 MHz, CD_3OD) δ 7.10 (d, *J* = 1.9 Hz, 1H), 6.84 (d, *J* = 1.9 Hz, 1H), 4.64 (dt, *J* = 11.5, 5.9 Hz, 1H), 4.01 (dd, *J* = 5.3, 1.2 Hz, 1H), 3.80 (d, *J* = 1.2 Hz, 1H), 2.79 (s, 3H), 2.64 (dd, *J* = 13.4, 6.3 Hz, 1H), 2.30 (dd, *J* = 13.4, 10 Hz, 1H) ppm. HRTOFMS [M − H]$^-$ *m/z* 339.0100 (calcd for $C_{12}H_{12}N_4O_3Br$, 339.0098).

13-Debromo-13-chloro-agelastatin A (1d).[23] *N*-Chlorosuccinimide (NCS, 5.0 mg, 38 μmoL, 2 equiv) and debromo-agelastatin A (1p, 5.0 mg, 19 μmoL, 1 equiv) were dissolved in water (0.38 mL, N_2 degassed), and the mixture treated with a solution of potassium persulfate (0.31 mg, 0.6 equiv) in degassed H_2O. The heterogeneous mixture was heated to 80 °C with vigorous stirring for 60 min. The mixture was allowed to cool to rt and was quenched with aqueous $NaHSO_3$ (50 μL of a 10% w/v solution), followed by neutralization with aqueous K_2HPO_4 (pH 9.5). The mixture was diluted with H_2O (1 mL) and extracted with *n*-BuOH (1.5 mL). The organics were concentrated under reduced pressure, and the residue purified by semipreparative reversed-phase HPLC (Luna phenyl−hexyl, 250 × 10 mm, 5 μm; linear gradient from 15−30% aqueous CH_3CN over 20 min, 2.5 mL min^{-1}), to yield 1d (t_R = 17 min, 2.2 mg, 39%), 1f (t_R = 20 min, 1.4 mg, 25%), and 1e (t_R = 27 min, 2.0 mg, 31%) as white solids. ^1H NMR (500 MHz, CD_3OD) δ 6.90 (d, *J* = 4.1 Hz, 1H), 6.23 (d, *J* = 4.1 Hz, 1H), 4.63 (dt, *J* = 12, 5.9 Hz, 1H), 4.08 (d, *J* = 5.5 Hz, 1H), 3.88 (s, 1H), 2.80 (s, 3H), 2.64 (dd, *J* = 13, 6.4 Hz, 1H), 2.11 (app-t, *J* = 12.6 Hz, 1H) ppm. HRTOFMS [M − H]$^-$ *m/z* 295.0604 (calcd for $C_{12}H_{12}N_4O_3Cl$, 295.0603).

13-Debromo-13,14-dichloro-agelastatin A (1e).[12] ^1H NMR (500 MHz, CD_3OD) δ 6.88 (s, 1H), 4.62 (dt, *J* = 12, 6.2 Hz, 1H), 4.10 (d, *J* = 5.5 Hz, 1H), 3.87 (s, 1H), 2.80 (s, 3H), 2.67 (dd, *J* = 13, 6.5 Hz, 1H), 2.14 (app-t, *J* = 12.6 Hz, 1H) ppm. HRTOFMS [M − H]$^-$ *m/z* 329.0215 (calcd for $C_{12}H_{11}N_4O_3Cl_2$, 329.0214).

13-Debromo-14-chloro-agelastatin A (1f).[12] ^1H NMR (500 MHz, CD_3OD) δ 7.07 (d, *J* = 1.7 Hz, 1H), 6.77 (d, *J* = 1.7 Hz, 1H), 4.62 (dt, *J* = 11.7, 6.0 Hz, 1H), 4.01 (dd, *J* = 5.2, 1.4 Hz, 1H), 3.79 (d, *J* = 1.4 Hz, 1H), 2.79 (s, 3H), 2.64 (dd, *J* = 13.4, 7.6 Hz, 1H), 2.30 (dd, *J* = 13.4, 10.1 Hz, 1H) ppm. HRTOFMS [M − H]$^-$ *m/z* 295.0604 (calcd for $C_{12}H_{12}N_4O_3Cl$, 295.0603).

13-Debromo-13-iodo-agelastatin A (1g). *N*-Iodosuccinimide (NIS, 1.9 mg, 9 μmoL, 1.5 equiv) and debromo-agelastatin A (1p, 1.5 mg, 6 μmoL, 1 equiv) were dissolved in dry DMF (0.1 mL) and stirred for 18 h at rt. An additional 1.3 mg (1.1 equiv) of NIS was added, and the reaction was allowed to continue for an additional 18 h. The reaction was then quenched with K_2CO_3 (10 μL satd aq), and the crude mixture purified by analytical reversed-phase HPLC (Luna phenyl−hexyl, 250 × 4.6 mm, 5 μm; linear gradient from 20−45% aqueous CH_3CN over 20 min, 0.7 mL min^{-1}), to yield 1g (t_R = 10 min, 0.6 mg, 21%), 1i (t_R = 14 min, 1.1 mg, 39%), and 1h (t_R = 20 min, 1.2 mg, 37%) as white solids. ^1H NMR (500 MHz, CD_3OD) δ 6.89 (d, *J* = 4.0 Hz, 1H), 6.47 (d, *J* = 4.0 Hz, 1H), 4.49 (dt, *J* = 12, 6.3 Hz, 1H), 4.05 (d, *J* = 5.7 Hz, 1H), 3.82 (s, 1H), 2.82 (s, 3H), 2.63 (dd, *J* = 12.7, 6.1 Hz, 1H), 2.04 (app-t, *J* = 12.7 Hz, 1H) ppm. HRTOFMS [M − H]$^-$ *m/z* 386.9961 (calcd for $C_{12}H_{12}N_4O_3I$, 386.9960).

13-Debromo-13,14-diiodo-agelastatin A (1h). ^1H NMR (500 MHz, CD_3OD) δ 7.07 (s, 1H), 4.54 (dt, *J* = 12.1, 6.0 Hz, 1H), 4.09 (d, *J* = 5.5 Hz, 1H), 3.87 (s, 1H), 2.82 (s, 3H), 2.69 (dd, *J* = 13, 6.5 Hz,

1H), 2.08 (app-t, J = 12.5 Hz, 1H) ppm. HRTOFMS [M − H]⁻ m/z 512.8928 (calcd for $C_{12}H_{11}N_4O_3I_2$, 512.8926).

13-Debromo-14-iodo-agelastatin A (1i). ¹H NMR (500 MHz, CD₃OD) δ 7.14 (d, J = 1.6 Hz, 1H), 6.93 (d, J = 1.6 Hz, 1H), 4.66 (dt, J = 9.8, 6.2 Hz, 1H), 3.99 (dd, J = 5.3, 1.4 Hz, 1H), 3.78 (d, J = 1.4 Hz, 1H), 2.79 (s, 3H), 2.62 (dd, J = 13.4, 6.5 Hz, 1H), 2.27 (dd, J = 13.3, 10.3 Hz, 1H) ppm. HRTOFMS [M − H]⁻ m/z 386.9963 (calcd for $C_{12}H_{12}N_4O_3I$, 386.9960).

13-Debromo-13-trifluoromethyl-agelastatin A (1j). To a solution of debromo-agelastatin A (**1p**, 6.0 mg, 23 μmol, 1 equiv) and sodium trifluoromethylsulfinate (3.6 mg, 69 μmol, 3 equiv) in water (50 μL) was added *tert*-butylhydroperoxide (70% w/v in water, 5.2 μL in 50 μL of H₂O, 5 equiv) very slowly without stirring at 0 °C. The reaction was allowed warm to rt and stirred for 24 h. The reaction was then quenched with sodium bicarbonate (50 μL satd aq). The organics were concentrated and the crude mixture purified by analytical reversed-phase HPLC (Luna C₁₈, 250 × 4.6 mm, 5 μm; linear gradient from 20−40% aqueous CH₃CN over 20 min, 0.7 mL min⁻¹) to yield **1j** (t_R = 19 min, 3.7 mg, 49%), **1l** (t_R = 20 min, 1.0 mg, 13%), and **1k** (t_R = 29 min, 2.3 mg, 25%) as white solids. For **1j**: [α]²⁵_D −68 (c 0.1, MeOH); UV (MeOH) λ_max (log ε) 240 (4.07), 260 (3.94); FTIR (ATR, ZnSe) ν_max 3265 (br), 1664, 1553, 1520, 1442, 1384, 1332, 1254, 1195, 1110, 757 cm⁻¹; ¹H NMR (500 MHz, CD₃OD) δ 6.92 (d, J = 4.1 Hz, 1H), 6.73 (d, J = 4.1 Hz, 1H), 4.59 (dt, J = 11.8, 5.9 Hz, 1H), 4.15 (d, J = 5.2 Hz, 1H), 3.90 (s, 1H), 2.78 (s, 3H), 2.66 (dd, J = 13.2, 6.3 Hz, 1H), 2.26 (app-t, J = 12.7 Hz, 1H) ppm; ¹³C NMR (125 MHz, CD₃OD) δ 161.4, 160.6, 127.3, 124.3, 121.0 114.1, 113.3 (q, J = 3.4 Hz), 95.4, 67.2, 62.2, 54.7, 41.0, 24.1 ppm; ¹⁹F NMR (470 MHz, CD₃OD) δ −60.5 ppm; HRTOFMS [M − H]⁻ m/z 329.0868 (calcd for $C_{13}H_{12}N_4O_3F_3$, 329.0867).

13-Debromo-13,14-ditrifluoromethyl-agelastatin A (1k). ¹H NMR (500 MHz, CD₃OD) δ 7.07 (s, 1H), 4.63 (dt, J = 11.8, 6.1 Hz, 1H), 4.20 (d, J = 5.3 Hz, 1H), 3.91 (s, 1H), 2.78 (s, 3H), 2.71 (dd, J = 13, 6.2 Hz, 1H), 2.35 (app-t, J = 12.7 Hz, 1H) ppm. ¹⁹F NMR (470 MHz, CD₃OD) δ −59.0, −60.7 ppm. HRTOFMS [M − H]⁻ m/z 397.0743 (calcd for $C_{14}H_{11}N_4O_3F_6$, 397.0741).

13-Debromo-14-trifluoromethyl-agelastatin A (1l). ¹H NMR (500 MHz, CD₃OD) δ 7.06 (d, J = 2.5 Hz, 1H), 6.49 (d, J = 2.5 Hz, 1H), 4.71 (dt, J = 11.4, 6.0 Hz, 1H), 4.02 (d, J = 4.9 Hz, 1H), 3.81 (s, 1H), 2.78 (s, 3H), 2.67 (dd, J = 13.3, 6.9 Hz, 1H), 2.30 (dd, J = 13.3, 10.3 Hz, 1H) ppm; ¹⁹F NMR (470 MHz, CD₃OD) δ −58.5 ppm; HRTOFMS [M − H]⁻ m/z 329.0867 (calcd for $C_{13}H_{12}N_4O_3F_3$, 329.0867).

13-Debromo-13-difluoromethyl-agelastatin A (1m). To a solution of debromo-agelastatin A (**1p**, 2.0 mg, 7.6 μmol, 1 equiv) and zinc difluoromethanesulfinate (DFMS, 4.5 mg, 15 μmol, 2 equiv) in water (50 μL) was very slowly added *tert*-butylhydroperoxide (70% solution in water, 3.14 μL in 50 μL of H₂O, 3 equiv) with vigorous stirring. The reaction was allowed to stir at rt for 20 h, and then second portions of DFMS (2 equiv) and ᵗBuOOH (3 equiv) were added. The reaction was allowed to stir for an additional 24 h, then quenched with sodium bicarbonate (50 μL). The organics were concentrated, and the crude mixture purified by analytical reversed-phase HPLC (Luna C₁₈, 250 × 4.6 mm, 5 μm; linear gradient from 15−40% aqueous CH₃CN over 15 min, 0.7 mL min⁻¹), to yield **1m** (0.7 mg, 29%) as a white powder. ¹H NMR (500 MHz, CD₃OD) δ 6.94 (dd, J = 53, 53 Hz, 1H), 6.88 (d, J = 4.0 Hz, 1H), 6.54 (m, 1H), 4.73 (m, 1H), 4.10 (d, J = 5.2 Hz, 1H), 3.88 (s, 1H), 2.79 (s, 3H), 2.70 (dd, J = 12.9, 6.3 Hz, 1H), 2.21 (app-t, J = 12.5 Hz, 1H) ppm. ¹⁹F NMR (470 MHz, CD₃OD) δ −112.2 (dd, J = 309, 55 Hz), −114.7 (dd, J = 308, 53 Hz) ppm. HRTOFMS [M − H]⁻ m/z 311.0958 (calcd for $C_{13}H_{13}N_4O_3F_2$, 311.0961).

13-Debromo-13-cyano-agelastatin A (1n). A flame-dried vial was charged with **1a** (5 mg, 15 μmol, 1 equiv), Zn(CN)₂ (1.4 mg, 12 μmol, 0.8 equiv), and Pd(PPh₃)₄ (1.7 mg, 1.5 μmol, 0.1 equiv), and purged with Ar. DMF (0.2 mL) was added, and the solution was allowed to stir at 95 °C for 24 h under Ar. The reaction was quenched with K₂CO₃ (10 μL satd aq), diluted with H₂O (0.5 mL), and extracted with n-BuOH (2 × 0.5 mL). The crude organics were concentrated and purified by semipreparative reversed-phase HPLC

(Luna phenyl−hexyl, 250 × 10 mm, 5 μm; linear gradient from 20−45% aqueous CH₃CN over 20 min, 2.5 mL min⁻¹) to yield **1n** (t_R = 10 min, 0.6 mg, 24% based on recovered starting material) and **1a** (t_R = 14 min) as white solids. ¹H NMR (500 MHz, CD₃OD) δ 6.94 (d, J = 4.2 Hz, 1H), 6.91 (d, J = 4.2 Hz, 1H), 4.76 (dt, J = 12, 6.3 Hz, 1H), 4.16 (d, J = 5.4 Hz, 1H), 3.89 (s, 1H), 2.82 (s, 3H), 2.71 (dd, J = 13.2, 6.6 Hz, 1H), 2.27 (dd, J = 12.5 Hz, 1H) ppm. HRTOFMS [M − H]⁻ m/z 286.0947 (calcd for $C_{13}H_{12}N_5O_3$, 286.0946).

14-Iodo-agelastatin A (1o). *N*-Iodosuccinimide (NIS, 12 mg, 52 μmol, 2 equiv) and agelastatin A (**1a**, 9.0 mg, 26.4 μmol, 1 equiv) were dissolved in dry DMF (0.2 mL) and stirred at rt for 24 h. An additional 2 equiv of NIS was added, and the reaction was allowed to continue for an additional 24 h. The reaction was then quenched with K₂CO₃ (50 μL satd aq), and the crude mixture purified by preparative reversed-phase HPLC (Duragel C₁₈, 50 × 20 mm, 5 μm; linear gradient from 25−50% aqueous CH₃CN over 20 min, 10 mL min⁻¹), to yield **1o** (11.4 mg, 92%) as a white solid. ¹H NMR (500 MHz, CD₃OD) δ 7.01 (s, 1H), 4.60 (dt, J = 12, 5.8 Hz, 1H), 4.08 (d, J = 5.3 Hz, 1H), 3.85 (s, 1H), 2.78 (s, 3H), 2.65 (dd, J = 13, 6.3 Hz, 1H), 2.09 (app-t, J = 12.5 Hz, 1H) ppm. HRTOFMS [M − H]⁻ m/z 464.9068 (calcd for $C_{12}H_{11}N_4O_3BrI$, 464.9065).

13-Debromo-agelastatin A (1p).[5b] A vial containing Pd−C (10%) (63 μg, 0.58 μmol, 0.1 equiv) and a solution of **1a** (10 mg, 29.3 μmol, 1 equiv) and dry triethylamine (16.4 μL, 0.117 mmol, 4 equiv) in MeOH (0.5 mL) was purged with H₂ and the contents stirred at rt under H₂ (1 atm) for 45 min. The reaction mixture was then passed through a 0.45 μm syringe filter, and after the removal of the volatiles, the residue was purified by preparatory reversed-phase HPLC (Duragel C₁₈, 50 × 20 mm, 5 μm; isocratic 1:9 CH₃CN/H₂O, 10 mL min⁻¹) to yield 13-debromo-agelastatin A (**1p**) as a white solid (7.2 mg, 90%), identical to that reported by Pietra and co-workers.[5b] ¹H NMR (500 MHz, CD₃OD) δ 7.03 (dd, J = 3.5, 1.5 Hz, 1H), 6.89 (m, 1H), 6.24 (m, 1H), 4.66 (dt, J = 11.5, 7.0 Hz, 1H), 4.00 (d, J = 5.0 Hz, 1H), 3.81 (s, 1H), 2.80 (s, 3H), 2.62 (dd, J = 13.4, 6.5 Hz, 1H), 2.28 (app-t, J = 11.9 Hz, 1H) ppm. HRTOFMS [M − H]⁻ m/z 261.0996 (calcd for $C_{12}H_{13}N_4O_3$, 261.0993).

13-Debromo-13-acetyl-agelastatin A (1q). To a solution of debromo-agelastatin A (**1p**, 1.5 mg, 5.7 μmol, 1 equiv) and sodium difluoroethanesulfinate (DFES, 2.6 mg, 17.2 μmol, 3 equiv) in H₂O (100 μL) was very slowly added *tert*-butylhydroperoxide (70% solution in water, 3.9 μL in 50 μL of H₂O, 5 equiv) with vigorous stirring. The reaction was allowed to stir at rt for 12 h and the mixture purified directly by analytical reversed-phase HPLC (Luna C₁₈, 250 × 4.6 mm, 5 μm; linear gradient from 15−40% aqueous CH₃CN over 15 min, 0.7 mL min⁻¹) to yield **1q** (1.0 mg, 58%) as a white powder. ¹H NMR (500 MHz, CD₃OD) δ 7.13 (dd, J = 4.1 Hz, 1H), 6.89 (d, J = 4.1 Hz, 1H), 5.33 (dt, J = 11.9, 5.8 Hz, 1H), 4.02 (d, J = 5.4 Hz, 1H), 3.87 (s, 1H), 2.86 (s, 3H), 2.78 (dd, J = 12.9, 6.4 Hz, 1H), 2.49 (s, 3H), 2.12 (app-t, J = 12.5 Hz, 1H) ppm. ¹³C NMR (600 MHz, CD₃OD, determined through HSQC and HMBC experiments) 191.4, 161.1, 160.8, 132.5, 128.2, 119.9, 113.7, 94.5, 67.1, 61.7, 54.4, 39.8, 27.3, 24.1 ppm. HRTOFMS [M + H]⁺ m/z 305.1247 (calcd for $C_{14}H_{17}N_4O_4$, 305.1244).

Resolution of (±)-Agelastatin A. Chiral phase HPLC resolution of synthetic (±)-agelastatin A **1a**[8b] (a generous gift from Professor Daniel Romo, Texas A&M University) was achieved using a Phenomenex Lux Cellulose-2 column (250 × 4.6 mm, 5 μm) under isocratic conditions (9:1 CH₃CN−i-PrOH and 0.1% Et₂NH, 1 mL min⁻¹). Natural (−)-agelastatin A (**1a**) eluted first (t_R = 19 min), followed by (+)-agelastatin A (**3**, t_R = 29 min). Enantiomeric purity was verified using CD spectroscopy (see Supporting Information, Figure S1).

***N,N,O*-Trimethyl-agelastatin A (4a).** The title compound was prepared according to the method of Pietra.[5b] Powdered KOH (12 mg) was added to a stirred solution of (−)-**1a** (1.0 mg, 2.9 μmol, 1 equiv) in DMSO (0.1 mL). After 10 min, excess iodomethane (9 μL, 50 equiv) was added, and the mixture stirred for an additional 30 min. The mixture was diluted with H₂O (1 mL), neutralized with satd NaH₂PO₄ (aq), and loaded onto a solvent prewashed reversed-phase cartridge (C₁₈, 0.2 g/3 mL) equilibrated with H₂O, then eluted with

H_2O (3 × 3 mL), followed by MeOH (3 × 3 mL). The methanol eluate was concentrated under reduced pressure to provide **4a** as a colorless amorphous solid (0.85 mg, 76%). ^1H NMR (500 MHz, CD_3OD) δ 6.89 (d, J = 4.0 Hz, 1H), 6.33 (d, J = 4.0 Hz, 1H), 4.68 (dt, J = 11.9, 5.9 Hz, 1H), 4.30 (s, 1H), 4.24 (d, J = 5.3 Hz, 1H), 3.18 (s, 3H), 3.14 (s, 3H), 2.98 (s, 3H), 2.81 (s, 3H), 2.68 (dd, J = 12.7, 6.7 Hz, 1H), 2.13 (app-t, J = 12.7 Hz, 1H) ppm. HRTOFMS $[M - H]^-$ m/z 383.0712 (calcd for $C_{15}H_{20}N_4O_3Br$, 383.0713).

***O*-Methyl-agelastatin A (4b).** A solution of (−)-**1a** (4.5 mg, 13.2 μmoL, 1 equiv) in MeOH (0.4 mL) was stirred with Amberlyst-15 resin for 18 h at 60 °C. The mixture was cooled to rt, filtered, and the filtrate concentrated and purified by semipreparative reversed-phase HPLC (Luna phenyl−hexyl, 250 × 10 mm, 5 μm; linear gradient from 20−60% aqueous CH_3CN over 20 min, 2.5 mL min^{-1}) to yield **4b**[5b] (3.5 mg, 74%) as a white solid. ^1H NMR (500 MHz, CD_3OD) δ 6.91 (d, J = 3.8 Hz, 1H), 6.33 (d, J = 3.8 Hz, 1H), 4.62 (dt, J = 11.7, 5.6 Hz, 1H), 4.12 (d, J = 4.7 Hz, 1H), 4.08 (s, 1H), 3.18 (s, 3H), 2.77 (s, 3H), 2.66 (dd, J = 13.1, 6.1 Hz, 1H), 2.14 (app-t, J = 12.7 Hz, 1H) ppm. HRTOFMS $[M - H]^-$ m/z 355.0404 (calcd for $C_{13}H_{16}N_4O_3Br$, 355.0400).

***O*-(2′-Methoxyethyl)-agelastatin A (4c).** A solution of (−)-**1a** (1.0 mg, 2.9 μmoL, 1 equiv) in 2-methoxyethanol (1 mL, distilled over 4 Å molecular sieves) was stirred with Dowex 50W-X8 (200−400 mesh, H$^+$ form, prewashed with 1 M HCl, rinsed with distilled H_2O, and dried) at 65 °C for 3 h under N_2, then overnight at rt. The mixture was filtered and the filtrate concentrated to yield **4c** (1.0 mg, 85%) as a white solid. ^1H NMR (500 MHz, CD_3OD) δ 6.92 (d, J = 4.1 Hz, 1H), 6.33 (d, J = 4.1 Hz, 1H), 4.62 (dt, J = 12.1, 6.0 Hz, 1H), 4.11 (d, J = 5.1 Hz, 1H), 4.10 (s, 1H), 3.56 (dt, J = 5.6, 3.2 Hz, 2H), 3.51 (dt, J = 10.2, 3.8 Hz, 1H), 3.39 (m, 1H), 3.37 (s, 3H), 2.80 (s, 3H), 2.68 (dd, J = 13.0, 6.6 Hz, 1H), 2.19 (app-t, J = 13.1 Hz, 1H) ppm. HRTOFMS $[M + Na]^+$ m/z 421.0483 (calcd for $C_{15}H_{19}N_4O_4BrNa$, 421.0482).

In Vitro CLL and HeLa Cell Line Assays. Primary leukemia cells from patients with CLL were obtained through the CLL Research Consortium. Institutional review board approval was obtained from the University of California, San Diego, and informed consent was obtained prior to the procurement of patient samples in accordance with the Declaration of Helsinki. Primary CLL cells or nonadherent cell lines (JVM-2) were cultured in RPMI (Cellgro, 10-040) with 10% fetal bovine serum (Gibco, 10099-141) and designated concentration of test compounds **1−4**. Following culture for 48 h (37 °C, 5% CO_2), viability was determined by fluorescence-activated cell sorting (FACS) analysis of mitochondrial membrane potential using 3,3′-dihexyloxacarbocyanine iodide (DiOC6) (Invitrogen/D-273) and cell membrane permeability to propidium iodide (PI) (Invitrogen, P1304MP). Cells were incubated with 40 nM DiOC6 and 10 μg/mL PI for 30 min at 37 °C and analyzed using a FACScalibur flow cytometer (Becton Dickinson). Fluorescence was recorded at 525 nm (FL-1) for DiOC6 and at 600 nm (FL-3) for PI. Relative viability was determined by calculating the percentage of the DiOC6 positive/PI negative population relative to an untreated or vehicle-treated control.

Viability of the adherent HeLa cell line was assayed by the MTT method. After incubation with test compounds **1−4**, media were replaced with 100 μL 0.5 mg/mL MTT (Sigma, M655) in RPMI without phenol red, and cells were incubated at 37 °C overnight, after which 25 μL of lysis buffer (15% SDS and 0.015 M HCl) was added to the cultures, and ODs at 570 nm were read once formazen was fully dissolved. EC_{50} values and standard errors (SEs) were calculated from dose−response curves using GraphPad Prism Software (La Jolla, San Diego).

Stability in Mouse/Human Plasma and Serum. Agelastatins **1a** or **1j** were added to 100 μL of mouse plasma or serum obtained and pooled from female BALB/c mice (Jackson Laboratory) to give a final compound concentration of 50 μM (1% DMSO) and incubated at 37 °C with gentle agitation. Time points (10 μL) were taken at t = 0, 0.5, 1, 2, 8, 18, and 24 h. The plasma/serum time point aliquots were treated as follows: proteins were precipitated in CH_3CN (100 μL), vortexed, and centrifuged at room temperature (3000g) for 10 min, and the supernatants were analyzed by LCMS. This procedure was repeated with human AB serum (Sigman/H4522). Stability tests were performed in triplicate.

Materials and Experimental Procedure for PK Study. BALB/c mice were obtained from Jackson Laboratory. At 6 weeks of age, agelastatins **1a** or **1j** were administered via an intraperitoneal (IP) route (2.5 or 5.0 mg/kg, n = 4). The blood samples were collected from the tail vein at the designated times. All biological specimens were stored at −80 °C until analysis.

Plasma PK Analyses. Blood samples were thawed and precipitated with CH_3CN (100 μL), vortexed, and centrifuged at room temperature (3000g) for 10 min. The samples were concentrated and reconstituted in 1:1 CH_3CN/H_2O (50 μL) for LCMS analysis. An internal standard (4,5-dibromo-*N*-propyl-pyrrole-2-carboxamide; 0.5 μg/mL) was added to all samples prior to analysis. An Agilent 6230 Accurate-Mass TOFMS LCMS system was used for sample analyses. Liquid chromatography was achieved with a Phenomenex Kinetex C_{18} column (150 × 4.6 mm, 2.6 μm) using gradient mobile phases of aqueous CH_3CN with 0.1% formic acid and a flow rate of 0.7 mL min^{-1}.

Phase I Metabolism Studies. Mouse (MSMC-PL) and human (HMMC-PL) microsomes were purchased from Life Technologies, and the assays were performed according to the manufacturer's protocol. Briefly, 100× stocks were prepared in DMSO for all test compounds (**1a**, **1j**, and **1p**) and controls (7-ethoxycoumarin). The final concentration of DMSO was <1%. The microsomes (20 mg/mL) were thawed slowly on ice. The following were added to each Eppendorf tube: 0.1 M sodium phosphate, pH 7.4 buffer (183 μL), microsomes (5 μL; final protein concentration = 5 mg/mL), and test compound (2 μL; final compound concentration = 100 μM). The mixture was preincubated at 37 °C for 5 min. The reactions were initiated upon the addition of NADPH (10 μL of a 20 mM solution in buffer; final concentration = 1 mM) and incubated for 60 min at 37 °C with gentle agitation. The reactions were terminated by the addition of MeOH (200 μL). The samples were vortexed and centrifuged at room temperature (3000g) for 5 min. The supernatant was removed and analyzed by LCMS. Controls included: zero time point with test compound; 60 min of incubation without NADPH, heat-inactivated microsomes (boiled at 100 °C for 15 min pretreatment); incubation with the CYP substrate 7-ethoxycoumarin.

Phase II Glucuronidation Metabolism Studies. Glucuronidation metabolism studies were performed with mouse (MSS9-PL) and human (HMS9-PL) S9 fractions purchased from Life Technologies. The procedure was performed as described by Fisher and colleagues.[18]

■ ASSOCIATED CONTENT

Ⓢ Supporting Information
CD and NMR spectra. This material is available free of charge via the Internet at http://pubs.acs.org.

■ AUTHOR INFORMATION

Corresponding Author
*Tel: +1-858-534-7115. Fax: +1-858-822-0386. E-mail: tmolinski@ucsd.edu.

Notes
The authors declare no competing financial interest.

■ ACKNOWLEDGMENTS

■ ABBREVIATION USED

PIA, pyrrole−imidazole alkaloids; CLL, chronic lymphocytic leukemia; SAR, structure−activity relationships; PK, pharmacokinetics; IV, intravenous; IP, intraperitoneal; AUC, area under curve; C_{max}, maximum compound concentration; T_{max}, time at which C_{max} occurs; $t_{1/2}$, half-life

■ REFERENCES

(1) Leukemia & Lymphoma Society, 2012. http://www.lls.org/diseaseinformation/getinformationsupport/factsstatistics/.

(2) Rogalinska, M.; Kilianska, Z. M. Targeting Bcl-2 in CLL. *Curr. Med. Chem.* **2012**, *19*, 5109−5115.

(3) Castro, J. E.; Melo-Cardenas, J.; Urquiza, M.; Barajas-Gamboa, J. S.; Pakbaz, R. S.; Kipps, T. J. Gene immunotherapy of chronic lymphocytic leukemia: a phase I study of intranodally injected adenovirus expressing a chimeric CD154 molecule. *Cancer Res.* **2012**, *72*, 2937−2948.

(4) Ross, D. D. Novel mechanisms of drug resistance in leukemia. *Leukemia* **2000**, *14*, 467−473.

(5) (a) D'Ambrosio, M.; Guerriero, A.; Debitus, C.; Ribes, O.; Pusset, J.; Leroy, S.; Pietra, F. Agelastatin A, A new skeleton cytotoxic alkaloid of the oroidin family - isolation from the Axinellid sponge *Agelas dendromorpha* of the Coral Sea. *J. Chem. Soc. Chem. Commun.* **1993**, 1305−1306. (b) D'Ambrosio, M.; Guerriero, A.; Chiasera, G.; Pietra, F. Conformational preferences and absolute configuration of agelastatin A, A cytotoxic alkaloid of the Axinellid sponge *Agelas dendromorpha* from the Coral Sea, via combined molecular modeling, NMR, and exciton splitting for diamide and hydroxyamide derivatives. *Helv. Chim. Acta* **1994**, *77*, 1895−1902. (c) Hong, T. W.; Jimenez, D. R.; Molinski, T. F. Agelastatins C and D, new pentacyclic bromopyrroles from the sponge *Cymbastela* sp., and potent arthropod toxicity of (−)-agelastatin A. *J. Nat. Prod.* **1998**, *61*, 158−161.

(6) Al-Mourabit, A.; Zancanella, M. A.; Tilvi, S.; Romo, D. Biosynthesis, asymmetric synthesis, and pharmacology, including cellular targets, of the pyrrole-2-aminoimidazole marine alkaloids. *Nat. Prod. Rep.* **2011**, *28*, 1229−1260.

(7) Stien, D.; Anderson, G. T.; Chase, C. E.; Koh, Y.-H.; Weinreb, S. M. Total synthesis of the antitumor marine sponge alkaloid agelastatin A. *J. Am. Chem. Soc.* **1999**, *121* (41), 9574−9579.

(8) (a) Duspara, P. A.; Batey, R. A. A short total synthesis of the marine sponge pyrrole-2-aminoimidazole alkaloid (±)-agelastatin A. *Angew. Chem. . Int. Ed.* **2013**, *52*, 10862−10866. (b) Reyes, J. C. P.; Romo, D. Bioinspired total synthesis of agelastatin A. *Angew. Chem., Int. Ed.* **2012**, *51*, 6870−6873. (c) Domostoj, M. M.; Irving, E.; Scheinmann, F.; Hale, K. J. New total synthesis of the marine antitumor alkaloid (±)-agelastatin A. *Org. Lett.* **2004**, *6*, 2615−2618. (d) Movassaghi, M.; Siegel, D. S.; Han, S. Total synthesis of all (−)-agelastatin alkaloids. *Chem. Sci.* **2010**, *1*, 561−566. (e) Wehn, P. M.; Du Bois, J. A stereoselective synthesis of the bromopyrrole natural product (−)-agelastatin A. *Angew. Chem. . Int. Ed.* **2009**, *48*, 3802−3805. For a comprehensive review of earlier agelastatin syntheses, see (f) Dong, G. Recent advances in the total synthesis of agelastatins. *Pure Appl. Chem.* **2010**, *82*, 2231−2314.

(9) Mason, C. K.; McFarlane, S.; Johnston, P. G.; Crowe, P.; Erwin, P. J.; Domostoi, M. M.; Campbell, F. C.; Manavazar, S.; Hale, K. J.; Ei-Tanani, M. Agelastatin A: a novel inhibitor of osteopontin-mediated adhesion, invasion, and colony formation. *Mol. Cancer Ther.* **2008**, *7*, 548−558.

(10) Meijer, L.; Thunnissen, A.; White, A. W.; Garnier, M.; Nikolic, M.; Tsai, L. H.; Walter, J.; Cleverley, K. E.; Salinas, P. C.; Wu, Y. Z.; Biernat, J.; Mandelkow, E. M.; Kim, S. H.; Pettit, G. R. Inhibition of

(11) Choi, M. Y.; Cardenas, J. M.; Lu, D. S.; Yu, J.; Stout, E. P.; Wu, R. P.; Horton, J. M.; Gomez, A.; Diaz-Perez, J. A.; Carson, D. A.; Molinski, T. F.; Kipps, T. J.; Castro, J. E. Agelastatin A, a marine sponge derived alkaloid, inhibits Wnt/β-catenin signaling and selectively induces apoptosis in chronic lymphocytic leukemia independently of p53. *Blood* **2011**, *118*, 779−779.

(12) Li, Z.; Shigeoka, D.; Caulfield, T. R.; Kawachi, T.; Qiu, Y.; Kamon, T.; Arai, M.; Tun, H. W.; Yoshimitsu, T. An integrated approach to the discovery of potent agelastatin A analogues for brain tumors: chemical synthesis and biological, physicochemical and CNS pharmacokinetic analyses. *Med. Chem. Commun.* **2013**, *4*, 1093−1098.

(13) Jones, P.; Koch, U.; Ontoria, J. M.; Scarpelli, R.; Schultz-Fademrecht, C. Preparation of 4-Oxo-4,5-dihydropyrrolo[1,2-a]-quinoxalines as Inhibitors of Poly(ADP-ribose)polymerase (PARP). PCT Int. Appl. 2007043677, 19 Apr, 2007.

(14) Nagib, D. A.; MacMillan, D. W. C. Trifluoromethylation of arenes and heteroarenes by means of photoredox catalysis. *Nature* **2011**, *480*, 224−228.

(15) (a) Ji, Y.; Brueckl, T.; Baxter, R. D.; Fujiwara, Y.; Seiple, I. B.; Su, S.; Blackmond, D. G.; Baran, P. S. Innate C-H trifluoromethylation of heterocycles. *Proc. Natl. Acad. Sci. U.S.A.* **2011**, *108*, 14411−14415. (b) Fujiwara, Y.; Dixon, J. A.; Rodriguez, R. A.; Baxter, R. D.; Dixon, D. D.; Collins, M. R.; Blackmond, D. G.; Baran, P. S. A new reagent for direct difluoromethylation. *J. Am. Chem. Soc.* **2012**, *134*, 1494−1497.

(16) This phenomenon was first observed by Baran and co-workers; see ref 15b.

(17) Wrighton, S. A.; Stevens, J. C. The human hepatic cytochromes P450 involved in drug metabolism. *Crit. Rev. Toxicol.* **1992**, *22*, 1−21.

(18) Fisher, M. B.; Campanale, K.; Ackermann, B. L.; Vandenbranden, M.; Wrighton, S. A. In vitro glucuronidation using human liver microsomes and the pore-forming peptide alamethicin. *Drug Metab. Dispos.* **2000**, *28*, 560−566.

(19) (a) Hansch, C.; Leo, A. *Substituent Constants for Correlation Analysis in Chemistry and Biology*; Wiley-Interscience: New York, 1979. (b) Hansch, C.; Leo, A.; Taft, R. W. A Survey of Hammett substituent constants and resonance and field parameters. *Chem. Rev.* **1991**, *97*, 165−195.

(20) (a) Uneyama, K. *Organofluorine Chemistry*; Blackwell: Oxford, U.K., 2006. (b) *Fluorine in Medicinal Chemistry and Chemical Biology*; Ojima, I., Ed.; Blackwell: Oxford, U.K., 2009. (c) MacPhee, J. A.; Panaye, A.; Dubois, J.-E. Steric effects: A critical examination of the Taft steric parameters. Definition of a revised, broader and homogeneous scale. Extension to highly congested alkyl groups. *Tetrahedron* **1978**, *34* (24), 3553−3562.

(21) The CHF_2 is only slightly less potent than CF_3, but here it is difficult to deconvolute the electron-withdrawing and steric effects.

(22) Wehn, P. M.; Du Bois, J. A Stereoselective synthesis of the bromopyrrole natural product (−)-agelastatin A. *Angew. Chem. Int. Ed.* **2009**, *48*, 3802−3805.

(23) At the time of this work, independent syntheses of **1d−f** were reported by Li and co-workers. See ref 12.

(24) Tilvi, S.; Moriou, C.; Martin, M.-T.; Gallard, J.-F.; Sorres, J.; Patel, K.; Petek, S.; Debitus, C.; Ermolenko, L.; Al-Mourabit, A. Agelastatin E, agelastatin F, and benzosceptrin C from the marine sponge *Agelas dendromorpha*. *J. Nat. Prod.* **2010**, *73*, 720−723.

■ NOTE ADDED IN PROOF

A publication on the cytotoxic activities of agelastatins A−F and synthetic intermediates has appeared. Han, S.; Siegel, D. S.; Morrison, K. C.; Hergenrother, P. J.; Movassaghi, M. Synthesis and Anticancer Activity of All Known (−)-Agelastatin Alkaloids. *J. Org. Chem.* **2013**, *78*, 11970−11984.